

Short Communication

Electrochemical nitrite nanosensor Based on Au Nanoparticles/Graphene Nanocomposites

Min Zhang^{1,2}, Faliang Cheng², Feng Gan^{1*}

¹School of chemistry and chemical engineering, Sun Yat-sen University, Guangzhou, Guangdong, 510275, China

²Dongguan University of Technology, Dongguan, Guangdong, 523808, China

*E-mail: cesgf@mail.sysu.edu.cn

Received: 28 February 2015 / Accepted: 14 April 2015 / Published: 27 May 2015

Au nanoparticles (AuNPs)/graphene nanocomposites has been fabricated and employed for the detection of nitrite. Morphological characterizations of nanocomposites showed that the Au nanoparticles were well dispersed on the graphene nanosheets surface with particle sizes of around 12 nm. Electrochemical investigations indicated that AuNPs/graphene nanocomposites electrode had high catalytic activity than the AuNPs on GCE and original GCE for the nitrite oxidation. Under the optimum conditions, the linear concentration dependences of peak current responses are observed for nitrite in the concentration ranges of $5.0 \times 10^{-5} \sim 5.1 \times 10^{-3}$ mol/L with the correlation coefficients of 0.998. The modified electrode has been used for determinations of nitrite in a real sample with satisfactory results.

Keywords: Nitrite; graphene; AuNPs; electrocatalytic oxidation

1. INTRODUCTION

Nitrite is a well-known alarming pollutant in our daily life because it is widely employed as an additive and corrosion inhibitor in food and environmental systems. It has been proved that excessive nitrite in the blood may lead to hemoglobin oxidation. Nitrite can react with amines to form carcinogens, N-nitrosamines. So, it is urgent to develop sensitive and accurate determination methods of nitrite. Up to now, many nitrite determination methods have been developed, such as chemiluminescence [1], spectrophotometry [2], and ion chromatography [3]. These methods are sensitive, but these methods require complicated instruments and time-consuming sample pre-treatment. Compared with these methods, the attractive electrochemical technique [4-5] shows rapid response, low cost, operational simplicity and high sensitivity. However, the redox reaction of nitrite

involves the large over-potential on bare solid electrodes, which limits the sensitive and selective detection of nitrite. Thus, to develop new materials to promote the electron transfer and to lower the operating potential for nitrite oxidation is considerable necessary[6-8].

Recently, two-dimensional nanomaterial graphene nanosheets have been extensively used in many fields due to its unique electronic properties [9-11]. As an ideal electrochemical material [12-13], graphene-based nanomaterials have captured wide attention from physicists, chemists, and material scientists. Among these graphene-based nanomaterials, various of catalytic nanoparticles (NPs) can be deposited on the graphene surface for the electrochemical sensing and detection. For example, graphene was employed as a Pt-Ru NPs support for the methanol electro-oxidation[14]. Li et al. [15] adopted gold NP modified graphene for the detection of enzymatic and Luan et al. adopted Au-graphene Graphene-HRP-chitosan biocomposites for the H₂O₂ detection [16]. However, the AuNPs/graphene nanocomposites have not been used for the detection of nitrite.

In this paper, AuNPs were deposited on graphene with sodium citrate as reductant and stabilizer through one-step reaction in solution. The peculiar structure of graphene allows for the configuration of scattered AuNPs on the surface of graphene. The cyclic voltammetry (CV) and chronoamperometry results also showed that the proposed sensor had a high sensitivity, excellent selectivity, and quick response for nitrite oxidation. Based on the experimental findings, a direct electrochemical method was developed to detect a real nitrite sample and achieved satisfactory detection results.

2. MATERIALS AND METHODS

2.1. Materials and reagents

The nitrite and HAuCl₄ (Sigma Chem. Co.) were of analytical reagent grade and purchased from Guangzhou Chemical Reagent Company. 0.1 mol/L PBS (pH=3.0) was used as the supporting electrolyte in all experiments. Doubly distilled deionized water from quartz was used throughout the work.

2.2. Apparatus

A PARSTAT 2273 electrochemical workstation (Princeton, USA) was used for amperometry measurements and cyclic voltammetry measurements at 25 °C. Pt electrode was employed as counter and Ag/AgCl (saturated KCl) was used as reference electrodes. Transmission electron microscope (TEM) analysis was performed with a JEM-2010HR (JEOL).

2.3. Preparation of electrodes

A glassy carbon electrode (GCE) was polished and thoroughly cleaned with alumina paste (Maruto, 1.0, 0.3, and 0.05). The AuNPs/Graphene/GCE was prepared according to the following

procedure. Firstly, the prepared GO [17-18] (2.5 mg) was dispersed in 10 mL of 0.5 mmol/L HAuCl_4 . Then, about 10.29 mL of 1% trisodium citrate solution was quickly added into the GO and HAuCl_4 mixture for 30-min intense stirring and the obtained solution was diluted to different volumes with doubly distilled deionized water. Finally, the modified electrode was achieved by depositing AuNPs/graphene on the cleaned GCE and then dried for 4 h in the air at 25 °C.

3. RESULTS AND DISCUSSION

3.1. TEM image of AuNPs/graphene composites

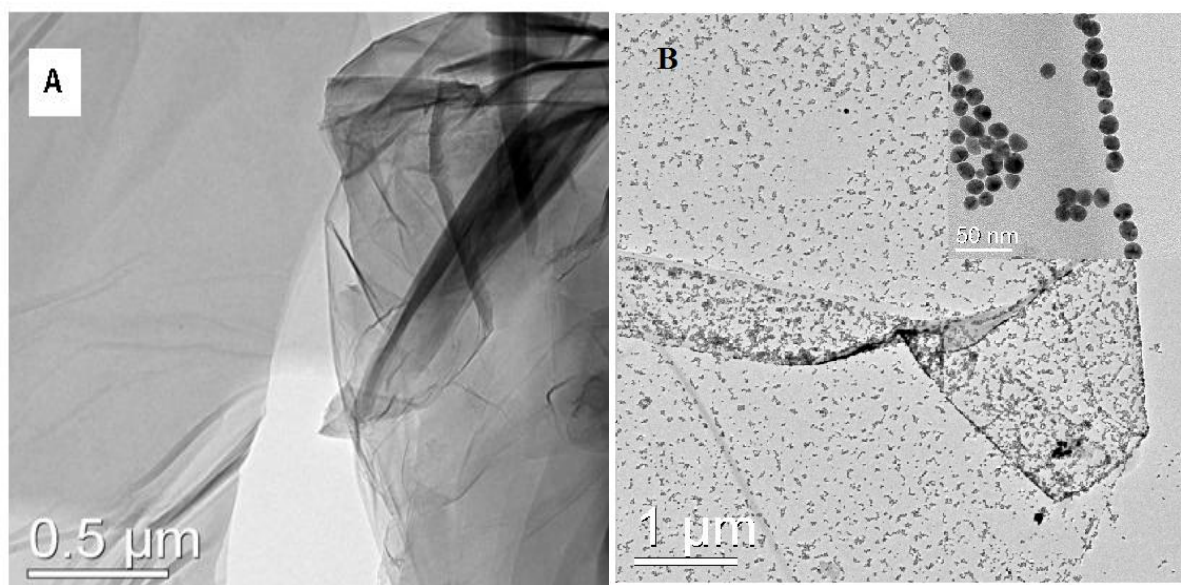


Figure 1. (A) TEM of graphene; (B) TEM of AuNPs/graphene (inset is 20 times magnification)

Fig. 1a shows the TEM image of graphene and the crumpled and wrinkled flake-like structure can be observed. The morphology of AuNPs/graphene composite was also investigated by TEM and shown in Fig. 1b. The AuNPs were homogeneously dispersed on the graphene sheet and the particles of AuNPs were mainly distributed on the surface of graphene and among the layers, indicating the good combination of graphene and AuNPs. The inset was the amplified AuNPs/graphene composite. Particles of AuNPs are spherical and the size of the spherical particles is around 12 nm.

3.2. Electrocatalytic behavior of nitrite on AuNPs/graphene/GCE

Fig. 2 represents the CVs of an unmodified GCE (a), an AuNPs electrode (b), and an AuNPs/graphene/GCE electrode (c). The CVs were recorded in a 5×10^{-3} mol/L nitrite in 0.1 mol L^{-1} PBS buffer solution.

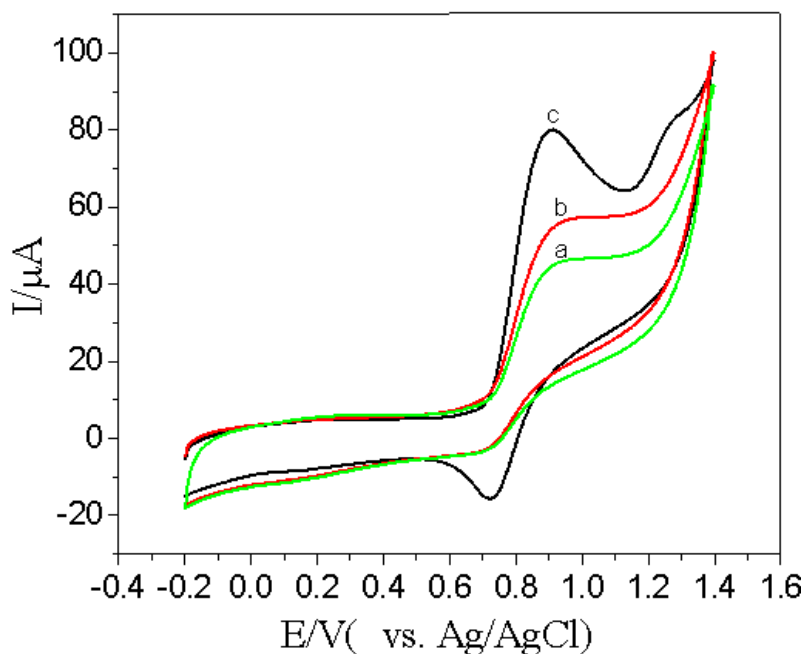


Figure 2. Cyclic voltammograms of unmodified GCE (a), an AuNPs electrode (b), and an AuNPs/Graphene/GCE (c) in $5 \times 10^{-3} \text{ mol L}^{-1}$ nitrite 0.1 mol L^{-1} PBS solution (pH 3.0) with a scan rate of 100 mV s^{-1} .

As shown in Fig. 2a, an irreversible and faint oxidation peak at 0.93 V observed on the unmodified GCE corresponds to the conversion from NO_2^- to NO_3^- . On the AuNPs/GCE, 0.92 V was the oxidation peak potential of nitrite and the current are slightly increased (Fig. 2b). However, for the AuNPs/graphene/GCE, the oxidation current is largest among those of bare GCE and AuNPs/GCE and the peak potential appears about 0.89 V. The high current responses at AuNPs/graphene/GCE to the electrooxidation of nitrite can be interpreted in the following three aspects. Firstly, the combination of graphene and the well dispersed ultrafine AuNPs provides larger electrochemically active surface area, which facilitates the adsorption of detected nitrite. Secondly, the AuNPs was interlocked on the “wrinkly” surfaces of graphene and so the interfacial electro-transfer process was greatly prompted. Thirdly, the high coverage of AuNPs and high conductivity of graphene can accelerate the electron transfer for nitrite oxidation.

3.3. Effects of pH

The effects of solution pH on the electrooxidation of nitrite at AuNPs/graphene/GCE was carefully investigated by cyclic voltammetry. It was showed that the peak currents increased with increasing pH value until it reaches 3.0, and then it decreased when the pH increases further. Therefore, the PBS buffer solution at pH 3.0 was chosen for the detection of nitrite.

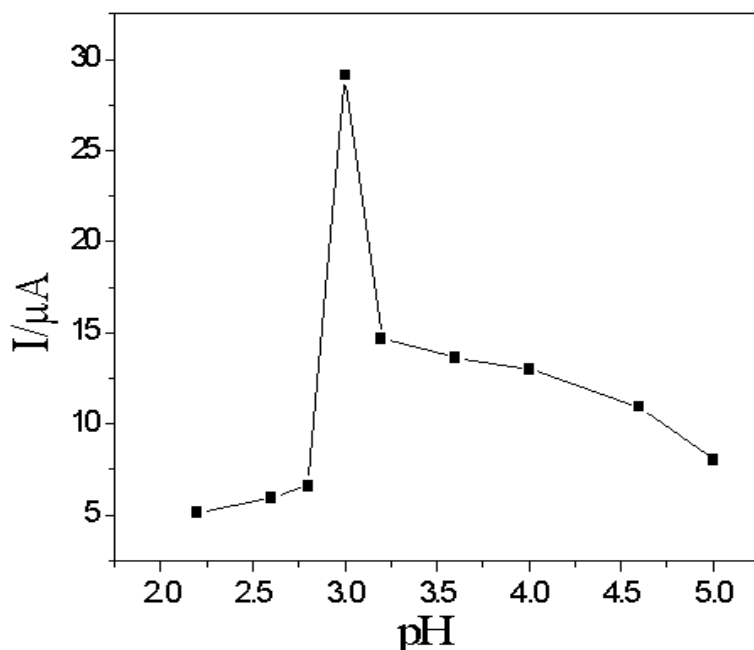


Figure 3. Effect of the pH value of 0.1 mol L^{-1} PBS solutions for $5 \times 10^{-3} \text{ mol L}^{-1}$ nitrite on AuNPs/graphene/GCE.

To obtain the kinetic parameters the cyclic voltammograms of AuNPs/graphene in the PBS solution at pH 3.0 in the presence of $5 \times 10^{-3} \text{ mol/L}$ nitrite were recorded at various scan rates (Fig. 4). With the increase of the scan rate, the oxidation peak current increased gradually and peak potential shifted to the left. The oxidation peak currents of nitrite were directly proportional to the square root of scan rate in the range from 10 to 300 mV s^{-1} as shown in Fig. 4B with the linear regression equations as: $I_{pa} (\text{mA}) = 16.93 + 90.38 v^{1/2}$ with $R^2 = 0.996$, indicating a diffusion-controlled process.

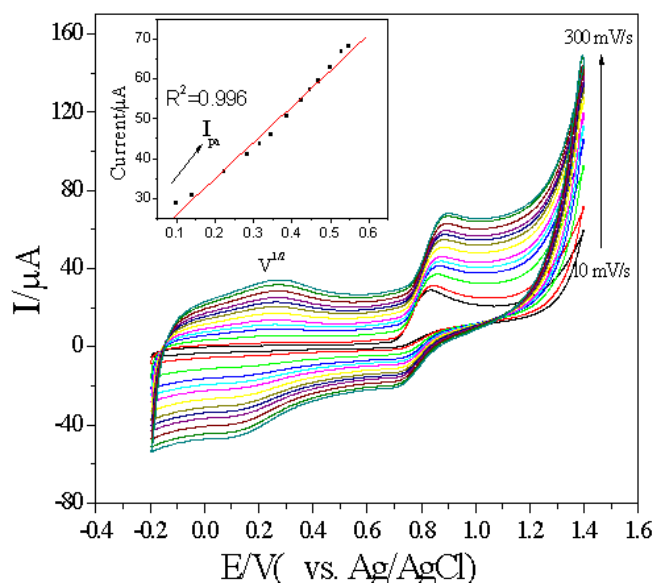


Figure 4. Cyclic voltammograms of the AuNPs/graphene/GCE in different scan rate of 10; 20; 50; 80; 100; 120; 150; 180; 200; 220; 250; 280; 300 mV/s. (inset: the relation of the anodic peak current for square root of scan rate)

3.4. Amperometric determination of nitrite using the sensor

Fig. 5 shows a typical amperometric response of the AuNPs/graphene/GCE to successive injections of nitrite into the stirred PBS (0.1 M, pH 3.0) at 0.89 V. A fast and obvious response was obtained after successive injecting of nitrite at the AuNPs/graphene/GCE. The oxidation currents were linear with the concentration of nitrite in the range of $5.0 \times 10^{-5} \sim 5.1 \times 10^{-3}$ M ($r = 0.998$), and the detection limit was 0.016 mM based on $S/N=3$. The comparison of this sensor with various other nitrite sensor was listed in Table 1 [20-26]. The results showed that this proposed method has the comparable low detection limits and wide linear ranges for determination.

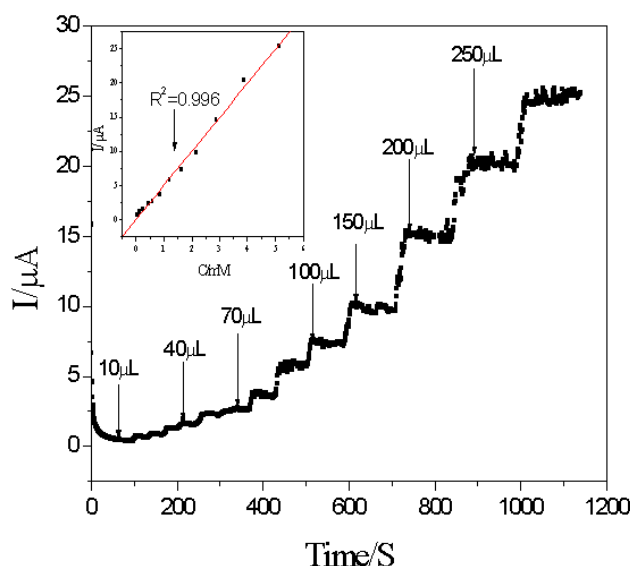


Figure 5. Amperometric response of the sensor to successive injection of nitrite into the stirred 0.1 M PBS at pH 3.0. (Inset: the plot of nitrite current versus its concentration)

Table 1. Comparison of various nitrite sensor

nitrite sensor	Linear range (M)	Detection limit (mM)	Reference
Pyridinium/Co-PcTs/SiO ₂ /SnO ₂ xerogel	4.0×10^{-5} to 1.7×10^{-3}	0.019	20
Platinum nanoparticles-modified GCE	1.0×10^{-5} to 1.0×10^{-3}	0.005	21
Ag nanoplates	1.0×10^{-5} to 1.0×10^{-3}	0.001	22
Cobalt nanoflowers	1.0×10^{-4} to 2.15×10^{-3}	0.001	23
Silica-cerium mixed oxide carbon paste electrode	3.0×10^{-5} to 3.9×10^{-3}	0.002	24
AuNP/glassy carbon electrode	1.3×10^{-4} to 4.4×10^{-2}	0.045	25
3-Methylpyridinium/SiO ₂ /SnO ₂ xerogel	1.3×10^{-5} to 1.3×10^{-3}	0.003	26
Ag NWs arrays/GCE	5.0×10^{-5} to 5.1×10^{-3}	0.016	This work

3.5. Reproducibility, stability, and interference

To characterize the repeatability of the sensor, successive determinations of nitrite were carried out. The relative standard deviation (RSD) of the sensor response to 5mM nitrite was 3.25% for 6 successive measurements. The operation stability of the AuNPs/graphene/GCE was also investigated. The AuNPs/graphene/GCE showed the 93.0% reproducibility after 7 days and 85% reproducibility after 2 months when stored at 4 °C.

Possible interference for the detection of nitrite on AuNPs/graphene/GCE was investigated by addition of various species into 0.1 M PBS solution (pH 3.0) containing 0.1 mM nitrite. The results showed that most of the ions, such as 100 times K^+ , Na^+ , Zn^{2+} , SO_4^{2-} , NO_3^- , HPO_4^{2-} , $H_2PO_4^-$, and glucose, did not interfere with nitrite determination.

3.6. Applications

we investigated the application of the proposed method for nitrite determination in the practical sausage samples. The crushed sausage (5.0 g) was added into 12.5 mL of saturated borax solution under stirring conditions. After 15-min heating at 100, 2.5 mL of 30% $ZnSO_4$ solution was dropped into the mixture and diluted to 500 mL. After the mixture stands for 10 min at the room temperature, the upper fat was discarded and the solution was filtered. Finally, the filtrate was mixed with 0.1 M PBS (pH 3.0) solution for detection. Recovery experiments were completed on the samples by adding nitrite standards solution (10^{-4} M). The obtained results are displayed in Table 2. The recovery was between 95 and 99.8% and the relative standard deviation of the three measurements was about 1.9-2.7, which proved that the electrode can be practically applied in determining of nitrite in real samples.

Table 2. Results for determination of nitrite in the real samples

Sample	Content (10^{-4} mol/L)	Added (10^{-4} mol/L)	Found (10^{-4} mol/L)	Recovery (%, n=3)	RSD (%, n=3)
1	1.104	1.00	2.012	99.8	2.7
2	0.655	1.00	1.605	95	2.3
3	0.419	1.00	1.401	98.2	1.9

4. CONCLUSION

This study provided a fast and simple way to fabricate an AuNPs/graphene/GCE with the one-step chemical reduction method. TEM results confirmed the combination of graphene and AuNPs. The prepared AuNPs/graphene/GCE exhibited excellent electrocatalytic activity for the nitrite oxidation.

The film shows high stability, good repeatability and anti-interference ability during the amperometric experiments. The high recovery showed that this simple and reliable method could probably be applied in the field of analysis and test.

ACKNOWLEDGMENTS

This work was supported by the National Natural Science Foundation of China (No. 20875106, 21375016, 21475022), Guangdong Natural Science Found Committee (9151027501000003), State Key Laboratory of Chemo/Biosensing and Chemometrics, Hunan University (4299001), the Natural Science Foundations of Guangdong Province (No.S2013010014324) and the Technology Project of Dongguan (2011108101016).

references

1. P. Mikuska, Z. Vecera, *Analytica Chimica Acta*, 495(2003)225.
2. M. N. Abbas, G. A. Mostafa, *Analytica Chimica Acta*, 410(2000)2185.
3. P. Niedzielski, I. Kurzyca, J. Siepak, *Analytica Chimica Acta*, 577(2006)220.
4. G. H. Lu, H. Jin, D. D. Song, *Food Chemistry*, 59(1997)583.
5. M. Bertotu, P. Derek, *Analytica Chimica Acta*, 337(1997)49.
6. Zh. H. Wen, T. F. Kang, *Talanta*, 62(2004)351.
7. J. Li, X. Q. Lin, *Microchemical Journal*, 87(2007)41.
8. T. Sh. Liu, T. F. Kang, L. P. Lu, Y. Zhang, Sh. Y. Cheng, *Journal of Electroanalytical Chemistry*, 632(2009)197.
9. K. S. Novoselov, A. K. Geim, S. V. Morozov, D. Jiang, Y. Zhang, S. V. Dubonos, I. V. Grigorieva, A. A. Firsov, *Science*, 306(2004)666.
10. V. C. Tung, L. M. Chen, M. J. Allen, J. K. Wassei, K. Nelson, R. B. Kaner, Y. Yang, *Nano Letters*, 9(2009)1949.
11. M. J. Allen, V. C. Tung, R. B. Kaner, *Chemical Reviews*, 110(2010)132.
12. V. Mani, A. P. Periasamy, Sh. M. Chen, *Electrochemistry Communications*, 17(2012)75.
13. J. F. Wu, M. Q. Xu, G. Ch. Zhao, *Electrochemistry Communications*, 12(2010)175.
14. Y. Wang, Y. Li, L. Tang, J. Lu, J. Li, *Electrochemistry Communications*, 11(2009)889.
15. S. Bong, Y. R. Kim, I. Kim, S. Woo, S. Uhm, J. Lee, H. Kim, *Electrochemistry Communications*, 12(2010)129.
16. K. F. Zhou, Y. H. Zhu, X. L. Yang, J. Luo, Ch. Z. Li, Sh. R. Luan, *Electrochimica Acta*, 55(2010)3055.
17. W. S. Hummers, R. E. Offeman, *Journal of America Chemistry Society*, 80(1958)1339.
18. N. I. Kovtyukhova, P. J. Ollivier, B. R. Martin, T. E. Mallouk, S. A. Chizhik, E. V. Buzaneva, A. D. Gorchinskiy, *Chemistry of Materials*, 11(1999)771.
19. S. Q. Liu, H. X. Ju, *Analyst*, 128(2003)1420.
20. M. Mir Reza, P. Azar, M. Hossein, S. Afsaneh, *Journal of the Chinese Chemical Society*, 62(2015)83
21. J. Arguello, H. A. Magosso, R. Landers, Y. Gushikem, *J Electroanal Chem*, 617(2008)45.
22. P. Miao, M. Shen, L. M. Ning, G. F. Chen, Y. M. Yin, *Analytical and Bioanalytical Chemistry*, 399(2011)407.
23. H. Helia, I. Eskandari, N. Sattarahmady, A. A. Moosavi-Movahedi, *Electrochimica Acta*, 77(2012) 294.
24. G. Silveira, A. d. Morais, P. C. M. Villis, C. M. Maroneze, Y. Gushikem, A. M. S. Lucho, F. L. Pissetti, *J. Colloid Interface Sci*, 369(2012) 302.
25. Y. Liu, H. Y. Gu, *Microchim Acta*, 162(2008)101.

26. J. Arguello, H.A.Magosso, R. Landers, V.L.Pimentel, Y. Gushikem, *Electrochimica Acta*, 56(2010)340.

© 2015 The Authors. Published by ESG (www.electrochemsci.org). This article is an open access article distributed under the terms and conditions of the Creative Commons Attribution license (<http://creativecommons.org/licenses/by/4.0/>).